Quaternary Science Advances 3 (2021) 100016

Contents lists available at ScienceDirect

Quaternary Science Advances

journal homepage: www.journals.elsevier.com/quaternary-science-advances

Persistent millennial-scale climate variability in Southern Europe during Marine Isotope Stage 6

G.P. Wilson [a,*], M.R. Frogley [b], P.D. Hughes [c], K.H. Roucoux [d], V. Margari [e], T.D. Jones [f], M.J. Leng [g,h], P.C. Tzedakis [e]

[a] Department of Geography & International Development, University of Chester, Chester, CH1 4BJ, UK
[b] Department of Geography, University of Sussex, Brighton, BN1 9QJ, UK
[c] Department of Geography, The University of Manchester, Manchester, M13 9PL, UK
[d] School of Geography & Sustainable Development, University of St Andrews, St Andrews, KY16 9AL, UK
[e] Environmental Change Research Centre, Department of Geography, University College London, London, WC1E 6BY, UK
[f] AECOM, Birmingham, B4 6AT, UK
[g] National Environmental Isotope Facility, British Geological Survey, Nottingham, NG12 5GG, UK
[h] School of Biosciences, University of Nottingham, Nottingham, LE12 5RD, UK

ARTICLE INFO

Keywords:
Marine Isotope Stage 6
Southern Europe
Millennial-scale climate variability

ABSTRACT

Exploring the mode and tempo of millennial-scale climate variability under evolving boundary conditions can provide insights into tipping points in different parts of the Earth system, and can facilitate a more detailed understanding of climate teleconnections and phase relationships between different Earth system components. Here we use fossil diatom and stable carbon and oxygen isotope analysis of lake sediment deposits (core I-284) from the Ioannina basin, NW Greece, to explore in further detail millennial-scale climate instability in southern Europe during Marine Isotope Stage 6 (MIS 6; ca. 185–130 ka). This interval correlates with the Vlasian Stage in Greece and the Late Saalian Substage in northern Europe, which were both characterised by extensive glaciations. The new dataset resolves at least 18 discrete warmer/wetter intervals, many of which were associated with strong Asian Monsoon events and North Atlantic interstadials. A number of cooler/drier intervals are also identified in the I-284 record, which are typically associated with weaker Asian Monsoon events and North Atlantic stadials, consistent with a variable Atlantic Meridional Overturning Circulation. Unlike the subdued changes in tree populations that are observed at Ioannina during mid-to-late MIS 6, the diatom record contains frequent high-amplitude oscillations in species assemblages, pointing to its sensitivity at a time when the lake system must have been close to environmental thresholds. Millennial-scale variability in diatom species assemblages continues into late MIS 6 at Ioannina, contributing important evidence for an emerging picture of frequent and persistent climate instability even at times of high global ice volume.

1. Introduction

Highly-resolved oxygen isotope ($\delta^{18}O$) analysis of Greenland ice cores reveal the existence of large magnitude changes in regional climate on millennial timescales during the last glacial period (Dansgaard et al., 1993). Although the exact cause of these so-called Dansgaard-Oeschger (D-O) cycles is unknown, there is now good evidence to suggest that many appear to coincide with significant changes in the Atlantic Meridional Overturning Circulation (AMOC), with a strengthening AMOC associated with D-O interstadials and a weakening AMOC associated with D-O stadials (Gottschalk et al., 2015; Henry et al., 2016; Lynch-Stieglitz, 2017). Conceptually, AMOC variability and its influence on the Intertropical Convergence Zone (ITCZ), for example via changes in North Atlantic sea ice extent (Kaspi et al., 2004; Chiang and Bitz, 2005; Li et al., 2005), provides a plausible unifying explanation for concomitant changes in climate beyond the North Atlantic (e.g. Wang et al., 2004; Broccoli et al., 2006; Tzedakis et al., 2009; Rhodes et al., 2015; Pedro et al., 2018; Corrick et al., 2020). 'D-O-type' millennial-scale climate oscillations also appear to be a feature of earlier glacial periods (McManus et al., 1999; Jouzel et al., 2007; Martrat et al., 2007), although their character and spatial expression are less well understood. It is important, therefore, to determine the presence, spatial expression and

* Corresponding author.
E-mail address: graham.wilson@chester.ac.uk (G.P. Wilson).

https://doi.org/10.1016/j.qsa.2020.100016
Received 7 September 2020; Received in revised form 20 October 2020; Accepted 6 November 2020
Available online 11 November 2020

regional character of D-O-type climate oscillations during earlier glacial episodes. Such knowledge will help us to refine our understanding of Earth system sensitivity and behaviour under differing orbital and ice sheet configurations.

During Marine Isotope Stage 6 (MIS 6; ca. 185–130 ka), which is defined as the Vlasian Stage in Greece (Hughes et al., 2006) and the western Balkans (Hughes et al., 2011), orbital and ice sheet configuration differed markedly from that of the Late Pleistocene last glacial cycle. In early MIS 6, precession minima and a highly eccentric orbit led to boreal summer (June) insolation values approaching 550 Wm^2 during MIS 6e (Berger, 1978), representing one of the most prominent (interstadial) insolation peaks of the Quaternary (Berger and Loutre, 1991). This was followed by one of the most extensive glaciations of the last 400 ka in Eurasia during the Late Saalian Substage (Ehlers et al., 2018). The maximum ice extent in Europe during the Late Saalian was reached relatively early during the Drenthe Stadial (ca. 170–155 ka) and preceded the global Penultimate Glacial Maximum at ca. 140 ka (Colleoni et al., 2016; Ehlers et al., 2018; Hughes and Gibbard, 2018). The Penultimate Glacial Maximum was associated with less extensive glaciation in Europe, during the Warthe Stadial, than during the Drenthe Stadial. The earlier, more extensive, Drenthe glacial limits in Germany are correlated with the maximum extent of ice cover in Britain in the Late Wolstonian (Gibbard et al., 2018) and with the Dnieper glaciation in Ukraine (Ehlers et al., 2013). The Dnieper ice lobe extended south of the Moscow glaciation limits, which are correlated with the Warthe Stadial (Ehlers et al., 2013). Some mid-latitude North Atlantic records reveal very high background concentrations of ice rafted debris (IRD) during MIS 6 (e.g. Obrochta et al., 2014), but unlike the coldest parts of the last glacial cycle (MIS 2–4), petrological evidence (detrital carbonate-rich 'Heinrich' deposits) for repeated surging of the Laurentide ice sheet through the Hudson straight is absent (Obrochta et al., 2014). Together with a range of geomorphological evidence (Hughes and Gibbard, 2018 and references therein) these observations are consistent with a different configuration and sensitivity of MIS 6 European and North American ice sheets compared to the last glacial cycle.

MIS 6 was punctuated by millennial-scale climate variability; in the North Atlantic region, this is reflected by Iberian Margin (MD01-2444) alkenone-derived sea-surface temperature (SST) reconstructions (Martrat et al., 2007). Further analysis of MD01-2444 by Margari et al. (2010) revealed deep-water hydrographic changes coincident with variations in Antarctic temperatures (Jouzel et al., 2007), suggesting an active Atlantic bi-polar see-saw during MIS 6. Pollen analysis of MD01-2444 and of core I-284 (Lake Ioannina, NW Greece) reveal particularly prominent increases in southern European tree populations during early MIS 6 North Atlantic interstadials (Margari et al., 2010; Roucoux et al., 2011). Based on the marine and terrestrial evidence contained in MD01-2444, Margari et al. (2010) distinguished between an earlier (185–155 ka) MIS 6 interval characterised by prominent millennial-scale variability, and a later interval (after 155 ka) characterised by relatively subdued, short-term variability, a pattern replicated in the I-284 arboreal pollen record (Roucoux et al., 2011). In Asia, Chinese speleothem $\delta^{18}O$ analysis reveals that millennial-scale strong Asian Monsoon events (Chinese Interstadials) took place throughout MIS 6 (Cheng et al., 2006). Infrequent but longer-duration strong Asian Monsoon events characterised the early part of MIS 6 prior to 160 ka, whilst up to 15 shorter-duration and smaller amplitude strong Asian Monsoon events are evident during the mid-late part of MIS 6 (Cheng et al., 2006; Wang et al., 2008, 2018). Stronger Asian Monsoons are thought to arise as a result of reduced North Atlantic sea-ice cover associated with a stronger AMOC, leading to a northward shift in the ITCZ over the Atlantic and the Pacific (Zhang and Delworth, 2005; Wang et al., 2018).

Whether mainland Europe experienced multiple equivalent interstadial events during mid-late MIS 6 remains unclear. The synthetic $\delta^{18}O$ record of Barker et al. (2011) does predict D-O-type warming events over Greenland continuing into the mid-late MIS 6, typically corresponding with strong Asian Monsoons (Wang et al., 2018) and weak South American Monsoons (Burns et al., 2019). Some mid-late MIS 6 climate variability is observed in European speleothem records (e.g. Regattieri et al., 2014; Koltai et al., 2017), but only restricted sections of MIS 6 are captured owing to growth interruptions. Only muted variability during the mid-late part of MIS 6 is suggested in the Southern European MD01-2444 and I-284 pollen records of tree populations (Margari et al., 2010, 2014; Roucoux et al., 2011), although variability in the abundance of specific taxa (*Artemisia* and Chenopodiaceae pollen in I-284, Ericaceae pollen in MD01-2444) and in the terrestrially-influenced Ca/Ti ratio (MD01-2444) appears more pronounced. This suggests that, with increasing global ice volume, mid-late MIS 6 southern European tree populations were sufficiently reduced such that their response to millennial-scale variability was muted. To help determine the character, spatial expression and frequency of millennial-scale climate events that influenced mainland Europe during MIS 6, we return to the core I-284 lake sediment sequence from Ioannina (Epirus, NW Greece; Fig. 1), and generate a highly resolved diatom and stable isotope ($\delta^{18}O$ and $\delta^{13}C$) record spanning the entire MIS 6 interval. Previous work on the I-284 sequence has revealed the sensitivity of these proxies to millennial-scale oscillations in hydro-climate at this site (Frogley et al., 2001; Tzedakis et al., 2003; Wilson et al., 2008, 2013, 2015; Jones et al., 2013).

2. Study area and methodology

The Ioannina basin is a polje thought to have formed during the Late Pliocene to Early Pleistocene (Clews, 1989). The basin is ca. 30 km long and up to 15 km wide, with a bedrock of Mesozoic and early Cenozoic limestones overlain by Pliocene and Quaternary lake sediment deposits. Artificial drainage has resulted in a reduced lake area of 22 km^2, with a mean water depth of 4–5 m (up to 11 m in places). Mt. Mitsikeli (1810 m above sea level, a.s.l.) forms the NW edge of the basin. To the SW, the topography slopes towards Mt. Tomaros (1974 m a.s.l.), and the Ionian Sea is located 40 km beyond (Fig. 1). Lake Ioannina forms the base level of a karst aquifer that underlies Mt. Mitsikeli. $\delta^{18}O$ and δD values of modern lake water demonstrate evaporative enrichment (Wilson et al., 2013), although the low mean water conductivity (0.3 mS cm^{-1}) is within the range of modern eutrophic waters and suggests that mechanisms currently exist which maintain a freshwater state (Wilson et al., 2008). The modern lake lacks a surface outflow; the freshwater state may therefore result from subterranean outflows via periodically unblocked sinkholes and/or natural outflows through small streams sinking beneath the limestone (Waltham, 1970). Lake Ioannina remained fresh throughout the Late Pleistocene to mid-Holocene despite fluctuations in level (Wilson et al., 2008; Jones et al., 2013), and glacial meltwater transfer to the subterranean karst system was identified as a plausible explanation for rapid lake level rise during the penultimate glacial-interglacial transition (MIS 6/5e boundary) (Wilson et al., 2015). Together, this underlines the long-term hydrological influence of groundwater in this karstic system, and the potential for groundwater throughflow.

Core I-284 (39°45′N, 20°51′E) from the Ioannina basin was recovered in 1989 by the Greek Institute of Geology and Mineral Exploration (IGME). The diatom, $\delta^{18}O$ and $\delta^{13}C$ records of the MIS 7/6 and 6/5e transitions are discussed in Frogley et al. (2001), Tzedakis et al. (2003) and Wilson et al. (2013, 2015). In this study, new samples for diatom and $\delta^{18}O$ and $\delta^{13}C$ analysis were taken at 20 cm intervals or greater (mean ca. 300-year resolution) between 102.2 m and 124.0 m and combined with existing data from the transition intervals to provide a continuous record of the entire MIS 6 interval. Preparation of samples for diatom analysis followed standard techniques, using hot H_2O_2 and HCl, with Naphrax™ as a slide mountant (Battarbee, 1986). Diatoms were analysed at x1000 and x1200 magnification, using a Leica LM1000 binocular microscope under phase contrast. Diatom preservation was sufficient to allow ≥500 valves to be counted in almost all samples analysed. Identification is based on Krammer and Lange-Bertalot (1986, 1988, 1991a, b) and Levkov et al. (2007), adopting current diatom nomenclature. Stratigraphical

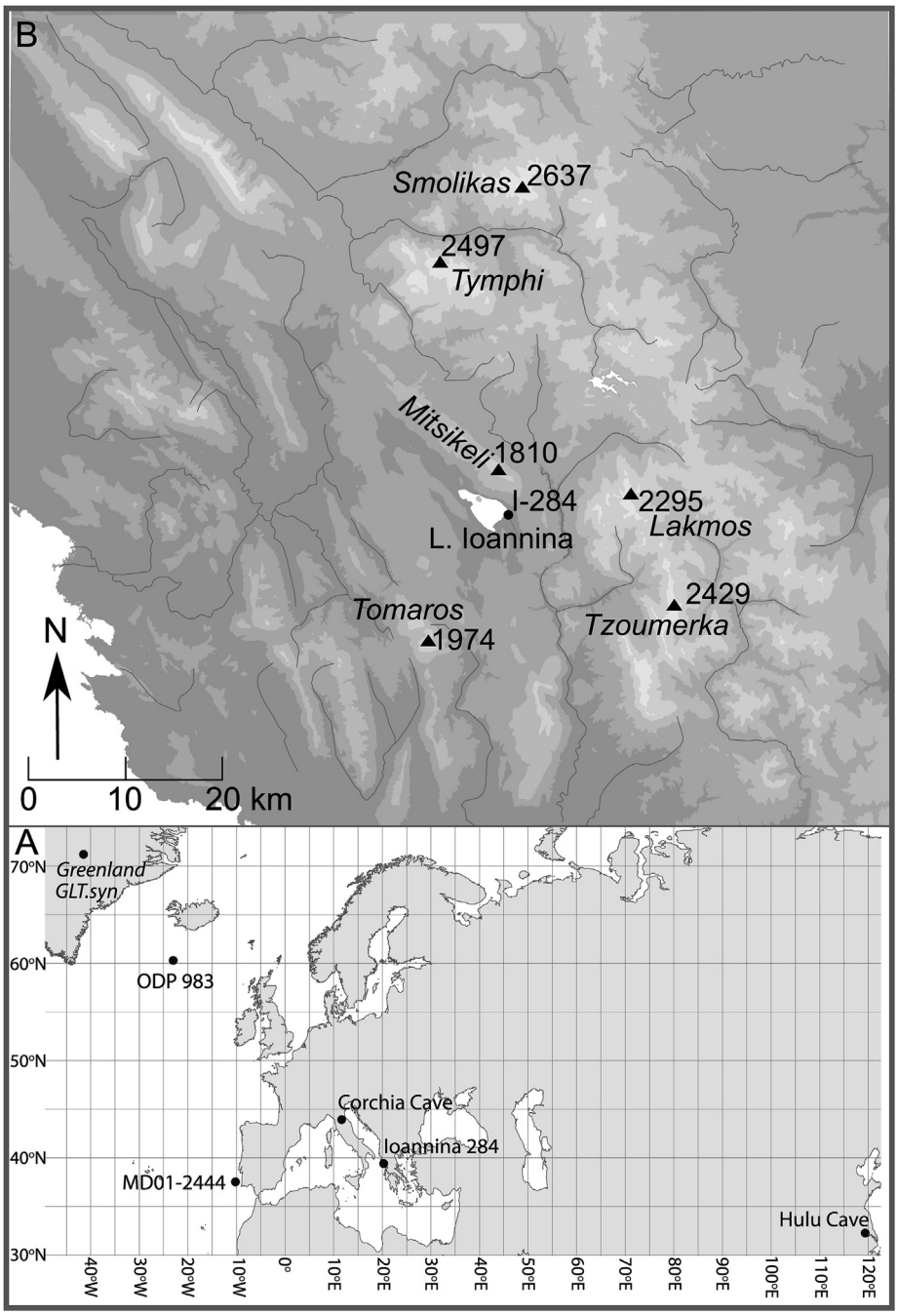

Fig. 1. A: Location of Ioannina (northwest Greece) and sites mentioned in the text. ODP 983—Ocean Drilling Program Site 983; *Greenland GLT.syn*—Greenland synthetic $\delta^{18}O$ record. B: Ioannina I-284 sediment core site (39°45′N, 20°51′E) in relation to the present lake (470 m above sea level) and surrounding topography. Adapted from Wilson et al. (2015).

zone boundaries were defined using CONISS (Grimm, 1987) on square-root transformed data (Fig. 2).

Volumetric (1 cm^3) sediment sub-samples were prepared for isotope analysis by disaggregation in 5% sodium hypochlorite solution for 24 h to oxidise reactive organic material and then washed 3x in distilled water. After sieving at 85 μm to remove faunal material, the resulting fine fraction was passed through Whatman QM-A quartz micro-filter paper, dried at 40 °C and then ground in an agate pestle and mortar. The isolated material was reacted with anhydrous phosphoric acid *in vacuo* overnight at a constant 25 °C; CO_2 liberated by this process was separated from water vapour and collected for analysis. Measurements were made on a VG Optima mass spectrometer at the National Environmental Isotope Facility in the UK; analytical reproducibility was <0.1‰ for both $\delta^{18}O$ and $\delta^{13}C$ (2σ). Previous work has determined that, in common with many Mediterranean lake systems, glacial $\delta^{18}O$ values at Ioannina are more enriched compared to interglacials (Tzedakis et al., 2003; Wilson et al., 2015), suggesting that temperature controls were less important drivers than evaporative and moisture source area changes. Accordingly, average glacial conditions in the catchment are interpreted as reflecting higher evaporation/precipitation (E/P) ratios than during interglacials. Notwithstanding the complex range of drivers influencing $\delta^{13}C$ values in lake waters, including organic productivity and source (Leng and Marshall, 2004), the likely role of E/P in also controlling $\delta^{13}C$ values at Ioannina is suggested by the general correspondence between the patterns of $\delta^{18}O$ and $\delta^{13}C$ (Tzedakis et al., 2003).

The MIS 6 age model follows Roucoux et al. (2011) by aligning the

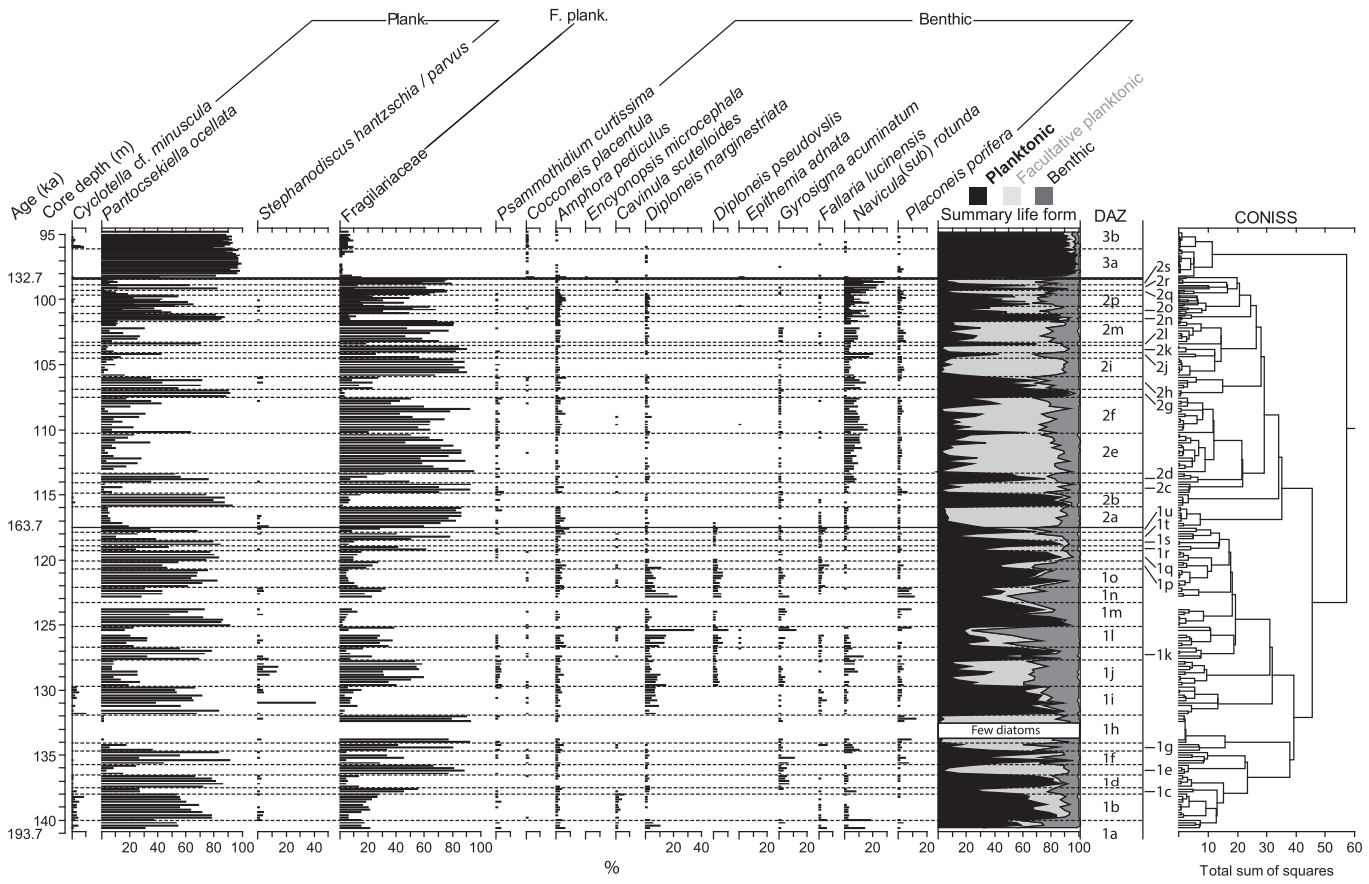

Fig. 2. I-284 diatom record showing taxa present at >2%, and summary life form. Frequencies of the facultative planktonics *Staurosirrella pinnata* [Ehrenberg] Williams and Round, *Straurosira construens* and *Pseudostaurosira brevistriata* [Grunow] Williams and Round are combined and expressed as Fragileraceae (%).

temperate tree pollen record in I-284 to that of marine core MD01-2444 on the western Iberian Margin (Margari et al., 2010) (Figs. 1 and 3), on the premise that millennial-scale SST variability in the North Atlantic and Mediterranean Sea leads to changes in evaporation and precipitation downstream in southern Europe, which in turn exerts a dominant influence over the composition of vegetation. A revised chronology for MD01-2444 (Margari et al., 2014) has been developed through alignment of its SST record with the Greenland synthetic record of Barker et al. (2011), itself aligned to precisely-dated Chinese speleothems (Cheng et al., 2009). The MD01-2444 chronology for the younger part of MIS 6 (139 ka onwards) is based on alignment to the Corchia Cave speleothem, Italy (Tzedakis et al., 2018, Fig. 1).

3. Results

Throughout the core sequence analysed, *Pantocsekiella ocellata* (Pantocsek) K.T. Kiss & Ács is the dominant planktonic species (Fig. 2), whilst the small Fragileraceae *Staurosirrella pinnata* [Ehrenberg] Williams and Round, *Straurosira construens* and *Pseudostaurosira brevistriata* [Grunow] Williams and Round together dominate the facultative planktonic habitat. The benthic community is more diverse, with species including *Amphora pediculus* [Kützing] Grunow, *Diploneis marginestriata* Hustedt, *Gyrosigma accuminatum* [Kützing] Rabenhorst, *Navicula rotunda* Hustedt and *Placoneis porifera* [Hustedt] Ohtsuka and Fujita. Three major biostratigraphic zones can be defined: diatom assemblage zone (DAZ) 1 (140.6–117.5 m, ca. 193.7–163.7 ka), DAZ 2 (117.5–98.23 m, ca. 163.7–132.7 ka) and DAZ 3 (98.23–95.02 m, ca. 132.7–127.5 ka). DAZ 3 spans the MIS 6/5 transition and is discussed in Wilson et al. (2015). DAZ 1 and DAZ 2 encompass MIS 6 (discussed here) and the transition from MIS 7 (Wilson et al., 2013). CONISS distinguishes two distinctive intervals in the MIS 6 diatom record (Fig. 2): an early MIS 6 interval (DAZ 1i to DAZ 1u; 131.9–117.5 m, ca. 178.0–163.7 ka) characterised by greater proportions of planktonic and benthic taxa, with a number of prominent oscillations in the percentage of *P. ocellata*; and a mid-late MIS 6 interval (DAZ 2a to DAZ 2s; 117.5–98.23 m, ca. 163.7–132.7 ka) characterised by an overall increase in small Fragilariaceae and punctuated by discrete episodes of planktonic expansion. In terms of stable isotope measurements from sediment calcite (Fig. 3), values of $\delta^{18}O$ oscillate markedly over the MIS 7/6 transition (values averaging ca. −2.3‰); for most of the subsequent MIS 6, however, values are lower on average (ca. −4‰) and are less variable. Values of $\delta^{13}C$ also oscillate distinctly across the MIS 7/6 transition, but then remain close to ca. 0‰ for most of the ensuing MIS 6.

4. Discussion

4.1. Early MIS 6

The peak boreal summer insolation maximum of the MIS 6e complex (centred at ca. 176 ka) is associated with a period of overall planktonic dominance between ca. 178 and 164 ka, and with some of the lowest $\delta^{18}O$ values recorded in the I-284 sequence, reaching < −7‰ at ca. 173 ka (Fig. 3). *P. ocellata* dominates the planktonic assemblages, a situation that is likely to reflect enhanced thermal stratification (Fahnenstiel and Glime, 1983; Winder et al., 2009) and lake deepening (Wilson et al., 2008, 2015; Jones et al., 2013). Extensive forest cover (Roucoux et al., 2011, Fig. 3) may have led to a reduction in catchment soil erosion and thus low sediment influx and lake turbidity, allowing the development of a diverse and extensive benthic habitat at the core site. Epipelic *Diploneis* and *Navicula* taxa are an important component of the benthos. These

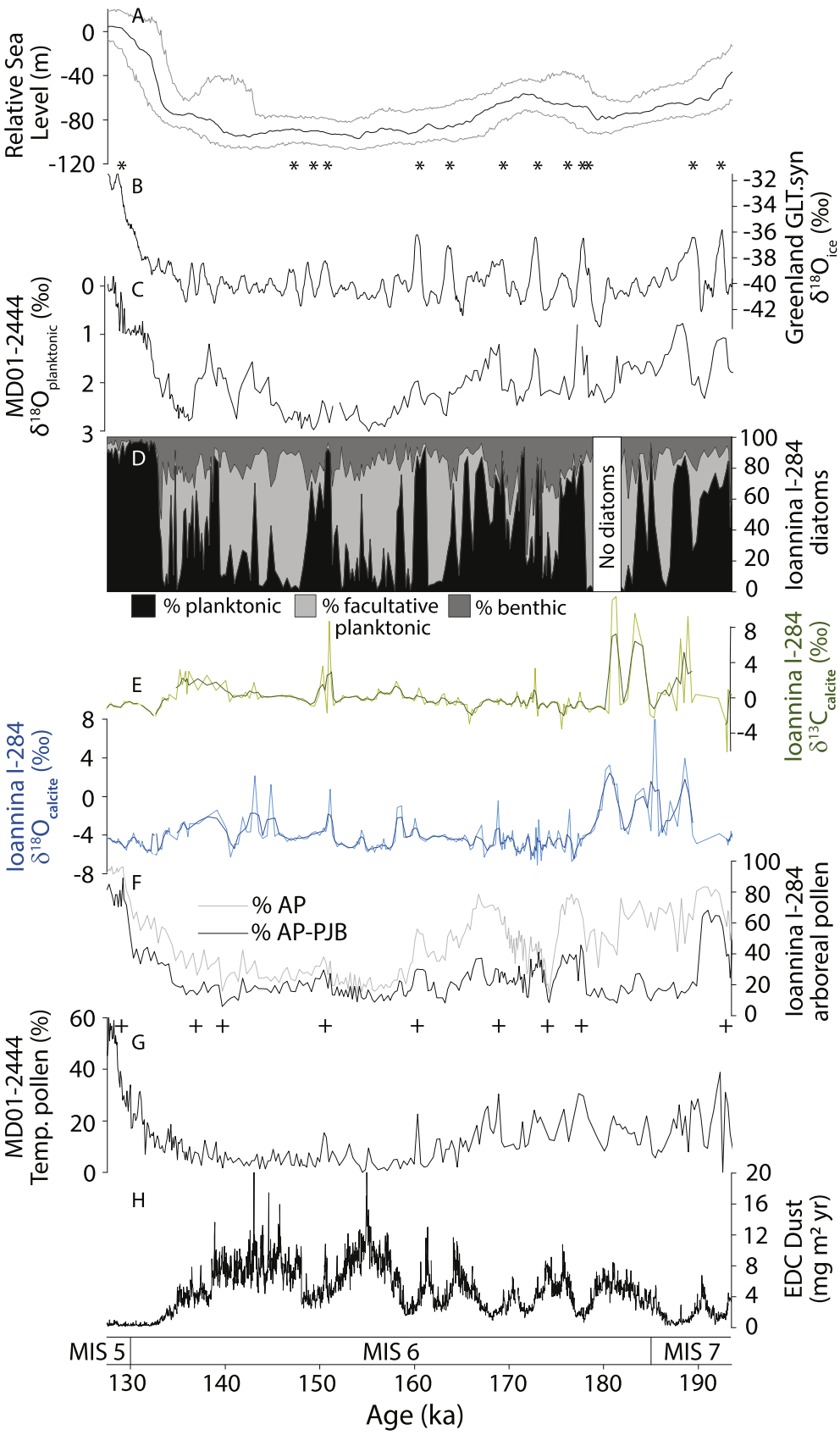

Fig. 3. (A) Red Sea sea-level, with 95% probability interval in light grey (Grant et al., 2014); (B) Greenland synthetic $\delta^{18}O$ record (Barker et al., 2011), with predicted D-O-type warming events denoted by *; (C) MD01-2444 (Portuguese Margin) $\delta^{18}O$ measured on specimens of planktonic *Globigerina bulloides* (Margari et al., 2010); (D) Ioannina I-284 diatom life form summary (this study); (E) Ioannina I-284 $\delta^{18}O_{calcite}$ (blue) and $\delta^{13}C_{calcite}$ (green) with 3 pt running mean (this study); (F) Ioannina I-284 % arboreal pollen (AP) and % arboreal pollen - *Pinus*, *Juniperus* and *Betula* (AP-PJB) (Roucoux et al., 2011); (G) MD01-2444 temperate pollen (%) (Margari et al., 2010), with age control points (denoted by +) used to construct the I-284 age model (see methods); (H) Antarctic EPICA Dome C dust flux (mg/m^2/yr) (Lambert et al., 2012).

actively motile taxa appear to exhibit a deeper water preference compared with araphid diatom species, such as the small Fragilariaceae *P. bevistriata*, *S. construens* and *S. pinnata*, which appear to prefer shallow water environments (Hoagland and Peterson, 1990; Wang et al., 2012). Lake deepening at Ioannina is consistent with existing evidence for increased regional precipitation during MIS 6e (e.g. Bard et al., 2002), likely to be in response to a northward migration of the ITCZ at times of precession minima and associated increased Mediterranean winter precipitation (Tzedakis et al., 2009; Bosmans et al., 2015; Wagner et al., 2019). Episodes of lake deepening and/or enhanced thermal stratification within the MIS 6e complex, inferred from *P. ocellata* dominance at ca. 178.0–175.3 ka (DAZ 1i), ca. 173.3–172.7 ka (DAZ 1k), ca. 169.5–166.4 ka (DAZ 1m–DAZ 1q), and ca. 165.7–165.1 ka (DAZ 1s) (Fig. 2) correspond to intervals of lower $\delta^{18}O_{planktonic}$ values (interstadials) in MD01-2444 (Portuguese Margin; Margari et al., 2010), strong Asian Monsoon events B17–B14 (Cheng et al., 2006; Wang et al., 2008), and predicted D-O-type interstadials (Barker et al., 2011) (Fig. 3). This adds support for a dynamic hydroclimate in Southern Europe during MIS 6e (Margari et al., 2010; Roucoux et al., 2011).

4.2. Mid-late MIS 6

There is a general increase in the percentage of facultative planktonic Fragilariaceae (typically >40%) and an overall reduction in benthic life

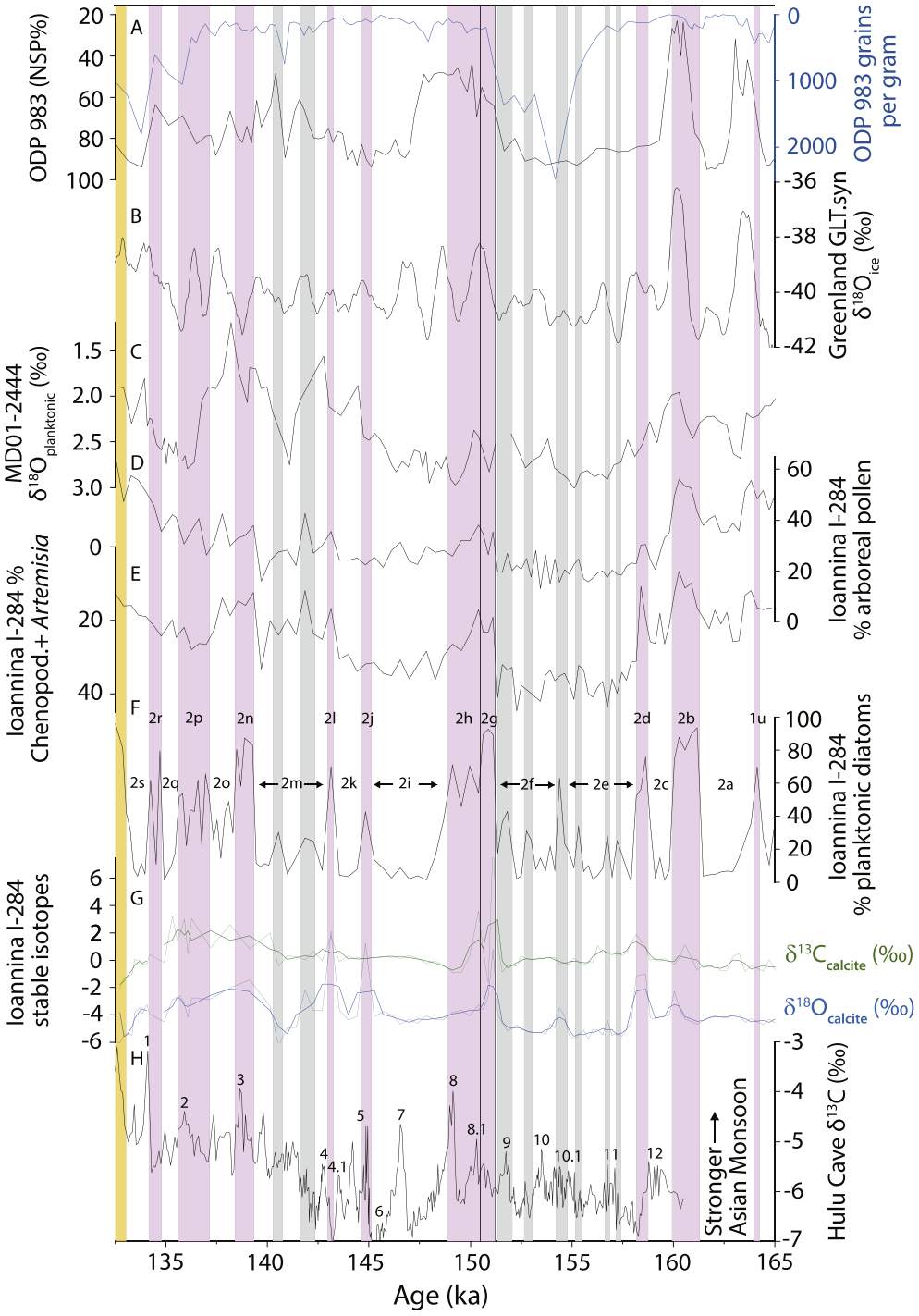

Fig. 4. (A) ODP 983 relative proportion of the polar planktonic foraminifera *Neogloboquadrina pachyderma* within the total assemblage, plotted alongside ODP 983 IRD grains per gram (Barker et al., 2015); (B) Greenland synthetic $\delta^{18}O$ record (Barker et al., 2011); (C) MD01-2444 (Portuguese Margin) $\delta^{18}O$ measured on specimens of planktonic *Globigerina bulloides* (Margari et al., 2010); (D) Ioannina I-284 tree pollen and (E) Chenopodiaceae + *Artemisia* (Roucoux et al., 2011); (F) Ioannina I-284 diatom planktonic frequencies (this study), with labelled DAZs. Time intervals where planktonic frequencies are elevated are shaded pink (distinctive biostratigraphical zones identified in cluster analysis) or olive (more conservative increases in planktonic frequencies of ≥20%), the orange shading identifies the onset of the transition to the Last Interglacial; (G) Ioannina I-284 stable isotope data, with 3 pt running mean (this study); (H) Hulu cave (China) speleothem $\delta^{13}C$ (Wang et al., 2018), with strong Asian Monsoon events (B1–B12) labelled. All data are plotted on their own time scales.

forms in mid-late MIS 6 (DAZ 2a to DAZ 2s; 117.5–98.23 m, ca. 163.7–132.7 ka) (Fig. 2). This is likely to be in response to lower overall boreal summer insolation, and is consistent with the approaching glacial maximum since the small Fragilariaceae *S. pinnata*, *S. construens* and *P. brevistriata* are characteristic of shallow lake conditions with extended seasonal ice cover in cold, arid glacial climates (Wilson et al., 2008, 2013, 2015; Jones et al., 2013). These small Fragilariaceae are extremely eurytopic and have been described as pioneering species (e.g. Haworth, 1976; Rawlence, 1992). They are common in shallow Arctic lakes (e.g. Douglas et al., 1994; Lotter et al., 1999; Laing and Smol, 2003) and in other lakes characterised by prolonged ice cover (Lotter and Bigler, 2000; Schmidt et al., 2004). They are able to tolerate unstable aquatic environments (Schmidt et al., 2004) characteristic of ice-covered lakes, where rapid changes in physical–chemical properties can occur during the melt period (e.g. in light penetration, temperature, nutrient concentrations: Ohlendorf et al., 2000; Schmidt et al., 2004). Changes in the proportion of facultative planktonic Fragilariaceae at Ioannina appear to have a close phase relationship with Antarctic dust flux (Fig. 3), and can be considered in the context of patterns of global and regional glaciation. Global patterns of glaciation can be inferred from polar dust records, which reflect the state of the global hydrological cycle (i.e. increased dust during more extensive glaciations reflecting increased global aridity as more freshwater is retained in ice masses). Dust flux over Antarctica has a close inverse relationship with air temperatures over the continent, with dust flux increasing as climate becomes colder (Lambert et al., 2008). Dust records are broadly mirrored in Greenland and Antarctic ice cores for the last glacial cycle (cf. Ruth et al., 2007; Lambert et al., 2012; Hughes et al., 2020, their Fig. 3) and thus, Antarctic dust records can be used as a proxy for global glaciations in earlier glacial cycles (Hughes et al., 2020, their Fig. 4). Furthermore, comparison of Antarctic ice-core dust records with loess/palaeosol sequences from the Chinese Loess Plateau (Kukla et al., 1994) confirms the synchronicity of global changes in atmospheric dust load (Lambert et al., 2008).

In MIS 6 two major phases of global glaciation can be identified in the Antarctic dust records, at ca. 157–152 ka and 148–138 ka (Fig. 3). In Europe, the maximum extent of glaciation in MIS 6, during the Drenthe Stadial, occurred after 163 ka (Margari et al., 2014). This correlates with the first phase of global glaciation. This maximum extent of European glaciation was the most extensive of the Pleistocene in the Netherlands and NW Germany (Ehlers et al., 2013). Ice was also more extensive over Britain in the Drenthe Stadial than during the Late Pleistocene Last Glacial Maximum (Gibbard et al., 2018). Such extensive ice cover would have caused dominant anticyclonic conditions over NW Europe and a blocking high (cf. Treidl et al., 1981), which is today associated with low precipitation over the southern Balkans (Lolis et al., 2012). Furthermore, glacial melting under rising boreal summer insolation (Toucanne et al., 2009) and consequent large seasonal discharges in the Fleuve Manche river (Channel River) (Eynaud et al., 2007), may have led to further aridity; associated advection of cooler surface waters to lower latitudes (Martrat et al., 2007) was cited as a possible explanation for the collapse of moisture-requiring temperate tree and Ericaceae populations in the western Mediterranean (Margari et al., 2014). Fragilariaceae expansion between ca. 158.1 ka and 151.3 ka (DAZs 2e and 2f in Figs. 2 and 4), as well as a shift to lower $\delta^{13}C$ and $\delta^{18}O$ values (consistent with low evaporation rates owing to cooler summers and extended seasonal lake ice cover; Ampel et al., 2010) and higher Chenopodiaceae and *Artemisia* abundance (Fig. 4), supports overall drier conditions in the Ioannina catchment (Roucoux et al., 2011) during the Drenthe Stadial. Whilst we interpret $\delta^{18}O$ values in Lake Ioannina as responding primarily to changing E/P, it is notable that values are generally low over this interval and are perhaps influenced in part by colder, more northerly air mass sources (Nagavciuc et al., 2019). Indeed, widespread cooling, particularly between ca. 157.9 and 154.6 ka, is apparent in central European speleothems (Koltai et al., 2017). Gulf of Lions SSTs are also lower at this time (Cortina et al., 2015). SSTs in this north-western part of the Mediterranean basin are strongly influenced by continental air masses, and particularly the intensity of cold north-westerly winds (from the Pyrenees, Massif Central and the Alps) which, in turn, are controlled by high-latitude dynamics (Cortina et al., 2015). Later glacial advances, during the Warthe Stadial (ca. 150–140 ka), were less extensive in Europe, where ice margins were 100–300 km and 600 km inside of the previous Drenthe Stadial glaciation in the west (Germany) and east (Russia/Belarus/Ukraine), respectively. Furthermore, whilst ice was present in the North Sea basin in the Drenthe, it was absent in the Warthe (Toucanne et al., 2009, their Figure 9) as well as from eastern England, where the Warthe Stadial was characterised by a periglacial environment (Gibbard et al., 2018). This corresponds to the second global glaciation indicated in the polar dust records and the global Penultimate Glacial Maximum. This is entirely consistent with the I-284 diatom record, as demonstrated by the second major expansion in Fragilariaceae (ca. 148.6–139.3 ka; DAZ 2i, 2k and 2m in Figs. 2 and 4), and is coincident with lower Alboran Sea and Iberian Margin SSTs (Martrat et al., 2004, 2007), indicating a return of prevailing aridity during the Warthe Stadial.

In addition to the Fragilariaceae increases during the Drenthe and Warthe Stadials, discrete Fragilariaceae expansion events appear to be associated with millennial-scale North Atlantic cold events. For example, Fragilariaceae expansion at ca. 142.6–139.5 ka (DAZ 2m; Figs. 2 and 4) is coeval with reduced SSTs and greater ice rafting in the North Atlantic (Barker et al., 2015; Deaney et al., 2017), termed Heinrich Stadial 12 by Lisiecki and Stern (2016). Additional Fragilariaceae expansion events at ca. 135.4–135.0 ka (DAZ 2q) and ca. 133.9–133.4 ka (DAZ 2s) coincide with Heinrich Stadials 11.1 and 11.2 (Tzedakis et al., 2018) and occur during weak Asian Monsoon intervals II-a and II-b, respectively (Wang et al., 2018), with DAZ 2s also coinciding with the onset of stadial conditions in central Europe (Koltai et al., 2017). Overall, the troughs in the proportion of planktonic diatoms and associated Fragilariaceae expansion events in mid-late MIS 6 (e.g. DAZ 2a, 2c, 2e, 2f, 2i, 2m, 2q, 2s), typically correspond with North Atlantic cold water-mass expansions and peaks in lithic and Icelandic volcanic glass concentrations (Obrochta et al., 2014; Barker et al., 2015), pointing to a link between millennial-scale North Atlantic variability and hydrological conditions in southern Europe.

The mid-late MIS 6 interval at Ioannina is punctuated with multiple episodes of often prominent increases in planktonic diatom frequencies. Although there is continued close correspondence between arboreal pollen and planktonic diatom frequencies in I-284, the differences in the amplitude of changes is striking (Fig. 4). The apparent sensitivity of the I-284 diatom record in particular provides an opportunity to further explore the character of mid-late MIS 6 climate in southern Europe. Cluster analysis of the I-284 diatom record identifies ten intervals characterised by high percentages of planktonic taxa (biostratigraphical DAZs 1u, 2b, 2d, 2g, 2h, 2j, 2l, 2n, 2p, 2r; highlighted with pink columns in Fig. 4), which punctuate mid-late MIS 6, with a further eight intervals of more minor, but nevertheless distinct, increases also apparent (planktonic taxa expansions of $\geq$20%; highlighted in olive-green in Fig. 4). Overall, the multiple episodes of often prominent increases in the planktonic species *P. ocellata* within mid-late MIS 6 are consistent with an interpretation of there being up to eighteen brief intervals between ca. 165 and 133 ka of enhanced lake thermal stratification (Fahnenstiel and Glime, 1983; Winder et al., 2009), a longer open-water season (Cremer and Wagner, 2003; Smol et al., 2005; Rühland et al., 2008) and perhaps higher (winter/spring) lake levels (Wilson et al., 2008, 2015; Jones et al., 2013). Several of the planktonic expansion events coincide with a shift to higher $\delta^{13}C$ and $\delta^{18}O$ values in particular (specifically at ca. 160.1 ka., 158.3 ka, 154.4 ka, 151.0 ka, 144.9 ka, 143.1 ka, 138.8 ka, 135.6 ka and 134.1 ka), suggesting both increased summer organic productivity and evaporative enrichment.

Planktonic diatom species expansion events in I-284 occur in association with a number of the interstadial events detected in other Northern Hemisphere records. Up to 15 strong Asian Monsoon (Chinese interstadial) events occurred in mid-late MIS 6, between 160.6 and 132.5 ka, as revealed in speleothem $\delta^{13}C$ and $\delta^{18}O$ records from Hulu Cave,

China (Wang et al., 2018), with climatic shifts also predicted in the Greenland synthetic $\delta^{18}O$ record (Barker et al., 2011). Specifically, core I-284 planktonic frequencies (and often E/P ratios) rise during eleven of the fifteen strong Asian Monsoon events (B1–B5, B8–B9, B10.1–B12), and during up to fifteen Greenland warm events predicted to have occurred between ca. 163.6 ka and 132.8 ka (Fig. 4). Several of the warming events identified in the I-284 record are resolved in SST records from the Iberian Margin (Martrat et al., 2007) and the Alboran basin (Martrat et al., 2004, 2014); SST changes in these locations are strongly influenced by North Atlantic oceanic conditions, particularly AMOC variability. For example, the abrupt and prominent SST warming event within the stadial associated with Heinrich event 11, first clearly observed in the Alboran basin ODP-976 sequence (Martrat et al., 2014), is also reflected in our I-284 diatom record (planktonic expansion event 2r, intercalated between the Fragilariaceae expansion events (2q and 2s in Fig. 4), together forming a 'double-u' shape reminiscent of the ODP-976 SST pattern (cf. Martrat et al., 2014)). In addition, slightly elevated annual mean SSTs in the Gulf of Lions, NW Mediterranean (Cortina et al., 2015), accompany most of the planktonic expansion events at Ioannina. Central European and Mediterranean speleothem records (e.g. Regattieri et al., 2014; Koltai et al., 2017; Nehme et al., 2018), which capture some intervals of MIS 6, resolve some of the millennial-scale events suggested by the diatom and isotope data during mid-late MIS 6. Episodes of planktonic expansion at ca. 164.1 ka (DAZ 1u) and at ca. 161.3–159.9 ka (DAZ 2b) are coeval (within dating errors) with wet intervals in the Levant (Nehme et al., 2018), and with warming in Central Europe at ca. 160 ka (Koltai et al., 2017). A shift to higher E/P ratios and a rise in planktonic diatom species frequencies at ca. 154.4 ka, which is associated with the strong Asian Monsoon event B10.1, is coeval with a central Europe interstadial (Koltai et al., 2017), and with wetter intervals in the Levant (Nehme et al., 2018). Further discrete increases in planktonic frequencies (and moderate shifts in E/P ratios) at ca. 139.2–138.5 ka (DAZ 2n), ca. 137.2–135.6 ka (DAZ 2p) and ca. 134.9–134.0 ka (DAZ 2r), which are associated with the strong Asian Monsoon events B1–B3, are coeval with warming events in central Europe (Koltai et al., 2017). An extended interval of planktonic dominance between ca. 151.3 and 148.8 ka (DAZ 2g and 2h) with associated high E/P ratios, may be a response to the small insolation maximum of the mid-late MIS 6 and occurs during the particularly strong Asian Monsoon events B8.1 and B8 (Fig. 4).

4.3. Emerging patterns and associated mechanisms

The I-284 diatom and $\delta^{18}O$ and $\delta^{13}C$ records demonstrate the persistence of millennial-scale climate variability in southern Europe throughout the entire MIS 6. Comparison of the Northern Hemisphere records considered above reveals that interstadial intervals of warmer North Atlantic and Mediterranean SSTs and stronger Asian Monsoon conditions are often associated with episodes of lake thermal improvement and perhaps deepening at Ioannina; conversely, stadial intervals of cooler North Atlantic and Mediterranean SSTs and weaker Asian Monsoons are often associated with colder and drier episodes with lake shallowing at Ioannina. A robust and consistent feature of several glacial climate model simulations, in which a freshwater flux (ranging between 0.1 and 0.4 Sv) is imposed in the North Atlantic, is cooling over the North Atlantic and much of extratropical Eurasia (projected mean annual surface air temperature fall of up to 7.5 K; Kageyama et al., 2013). These same models also predict that freshwater input to the North Atlantic, for instance due to sea-ice expansion or iceberg discharges, would result in a corresponding fall in mean annual precipitation over the North Atlantic, and typically extending into Europe. North Atlantic extended sea-ice, and surface ocean cooling in both the North Atlantic and Mediterranean (Martrat et al., 2004, 2007), would result in lower evaporation rates and reduced rainfall, as well as altered atmospheric circulation patterns, promoting enhanced aridity in Southern Europe during D-O-type stadials. In the I-284 record, expansion in small Fragilariaceae taxa characteristic of shallow lake conditions with extended seasonal ice cover (Wilson et al., 2008, 2013, 2015; Jones et al., 2013), as well as low E/P ratios, presumably reflecting suppression of summer evaporation, are consistent with this modelled climatic scenario.

At Ioannina, intervals with an increased percentage of diatom planktonic taxa, as determined by cluster analysis, and intervals of higher E/P (for the most part) occur during the predicted warming events of Barker et al. (2011) (Figs. 3 and 4), providing support for their synthetic Greenland record. These predicted warming events imply episodic enhanced cross-equatorial heat transport into the North Atlantic via the AMOC during MIS 6, and Margari et al. (2010) found evidence consistent with an active Atlantic bi-polar seesaw. Moreover, as interstadials are associated with a northward migration of the ITCZ (with stronger Asian Monsoons and weaker South American monsoons) and stadials associated with a southward migration of the ITCZ (with weaker Asian Monsoons and stronger South American Monsoons) (Wang et al., 2004; Rhodes et al., 2015; Corrick et al., 2020), similar antiphasing in Asian and South American monsoon strength during MIS 6 (Wang et al., 2018; Burns et al., 2019) is consistent with episodes of enhanced cross-equatorial heat transport, presumably in association with a strengthening AMOC. Corresponding warmer North Atlantic and Mediterranean SSTs (Martrat et al., 2004, 2007) would be expected to lead to greater (winter) precipitation in Southern Europe, presumably linked to higher Mediterranean SSTs lasting into the autumn, leading to enhanced winter air-sea surface temperature gradients and promotion of convective (winter) rainfall (Bosmans et al., 2015). At Ioannina, planktonic habitat expansion events (many coinciding with reduced Chenopodiaceae and *Artemisia* pollen abundance in I-284 (Roucoux et al., 2011, Fig. 4) and with elevated North Atlantic and Mediterranean SSTs (Martrat et al., 2004, 2007, 2014; Cortina et al., 2015) may reflect elevated water levels following wetter winters, whilst warmer and drier summers suggested by elevated E/P ratios, would also enhance summer thermal lake stratification and thus dominance by *P. ocellata*.

At Ioannina, reconstructed millennial-scale events tend to be more frequent and brief (<1 ka) during mid-late MIS 6 (ca. 163–133 ka), and less frequent and longer (ca. >2 ka) in duration in early MIS 6 (ca. 185–163 ka), a pattern consistent with MD01-2444 (Margari et al., 2010) and the Chinese speleothem record (Wang et al., 2008). The reduced amplitude and duration of mid-late MIS 6 interstadials apparent in a number of records (e.g. Margari et al., 2010; Roucoux et al., 2011), may reflect an overall weakening of the millennial-scale climate variability (Margari et al., 2010, 2014) as global ice volumes exceeded a critical threshold (McManus et al., 1999; EPICA Community Members, 2006). The numerous distinct discrete planktonic expansion events at Ioannina are often associated with only relatively small increases in arboreal populations, and intervals of elevated E/P ratios are not accompanied by any significant expansion of Mediterranean elements in the vegetation (Roucoux et al., 2011), together suggesting that any increase in winter precipitation and in summer temperatures and/or aridity was relatively minor compared with those changes experienced in early MIS 6. The differences in the amplitude of response of arboreal pollen and planktonic diatom frequencies to common climatic forcing events appears to point to differences in lacustrine and terrestrial thresholds of response. The subdued oscillations in arboreal pollen reflect the combined effects of reduced precipitation and winter temperatures, a shorter growing season and also lower atmospheric CO_2 concentrations, which led to tree population contraction (but not their complete elimination) across the mid-late MIS 6 interval (Tzedakis et al., 2002; Roucoux et al., 2011). As discussed in Wilson et al. (2013), diatoms can be highly responsive to environmental change when lake physical–chemical thresholds are approached and exceeded, and this is particularly apparent in lakes associated with snow and ice cover. Slight warming resulting in decreased lake ice cover will affect the length of the growing season, E/P ratios (as reflected by stable isotopic values), the thermal regime of the lake, and a range of chemical variables (e.g. Ohlendorf et al., 2000), which can lead to pronounced changes in diatom species assemblages.

Indeed, this has been recorded in many high latitude and temperate lakes in response to contemporary (post-industrial) warming (Smol et al., 2005). It follows that large changes in diatom species assemblages may occur as a result of relatively small forcing events when the lake system is close to an environmental threshold (Rühland et al., 2015). In such a context, diatoms will be sensitive to subtle changes in climate that may produce smaller responses in other ecosystems and their proxies.

In contrast with the coldest parts of the last glacial cycle (MIS 2–4) and the antepenultimate glacial cycle (MIS 8), Obrochta et al. (2014) found that MIS 6 contained nearly continuously elevated concentrations of lithic IRD grains, especially after ~160 ka, in North Atlantic core U1308; elevated lithic concentrations were found in MIS 6 sediments in nearby V28-82 (Downing, 2008) and in core M23124 from the Rockall Plateau (Didié and Bauch, 2000), but lower concentrations characterised the eastern Atlantic ODP 980 sequence (McManus et al., 1999), which may suggest altered circulation patterns (Obrochta et al., 2014). The high background concentrations of IRD observed in North Atlantic cores U1308, V28–82 and M23124 would indicate near continuous freshwater fluxes, which may have increased AMOC disruption sensitivity to relatively weak, or well-placed, forcing events (Margari et al., 2010). The evidence from Ioannina, combined with records of changes in North Atlantic and Asian conditions, demonstrate that millennial-scale variability characterised the entire MIS 6, and contribute to an emerging picture of frequent and persistent (but subdued) climate instability even at times of higher global ice volume.

Declaration of competing interest

The authors declare that they have no known competing financial interests or personal relationships that could have appeared to influence the work reported in this paper.

Acknowledgements

We thank Phil Gibbard, University of Cambridge, and Editor Neil Glasser, University of Aberystwyth, for providing thorough reviews of this paper. GW gratefully acknowledges the financial support provided by The University of Chester. Isotope analyses were undertaken at the National Environmental Isotope Facility, UK. We are grateful to IGME for providing access to core I-284, and to NERC and the University of Cambridge for facilitating the transport of the core to the UK. Stephen Barker, Gabriella Koltai, Carole Nehme, Eleonora Regattieri and Quan Wang are thanked for kindly sharing their data.

References

Ampel, L., Wohlfarth, B., Risberg, J., Veres, D., Leng, M.J., Tillman, P.K., 2010. Diatom assemblage dynamics during abrupt climate change: the response of lacustrine diatoms to Dansgaard-Oeschger cycles during the last glacial period. J. Paleolimnol. 44, 397–404.

Bard, E., Delaygue, G., Rostek, F., Antonioli, F., Silenzi, S., Schrag, D.P., 2002. Hydrological conditions over the western Mediterranean basin during the deposition of the cold Sapropel 6 (ca. 175 kyr BP). Earth Planet Sci. Lett. 202, 481–494.

Barker, S., Chen, J., Gong, X., Jonkers, L., Knorr, G., Thornally, D., 2015. Icebergs not the trigger for North Atlantic cold events. Nature 520, 333–336.

Barker, S., Knorr, G., Edwards, R.L., Parrenin, F., Putnam, A.E., Skinner, L.C., Wolff, E., Ziegler, M., 2011. 800,000 years of abrupt climate variability. Science 334, 347–351.

Battarbee, R.W., 1986. Diatom Analysis. In: Berglund, B.E. (Ed.), Handbook of Holocene Palaeoecology and Palaeohydrology. Wiley, Chichester, UK, pp. 527–570.

Berger, A., 1978. Long-term variations of caloric insolation resulting from the Earth's orbital elements. Quat. Res. 9, 139–167.

Berger, A., Loutre, M.F., 1991. Insolation values for the climate of the last 10 million years. Quat. Sci. Rev. 10, 297–317.

Bosmans, J.H.C., Drijfhout, S.S., Tuenter, E., Hilgen, F.J., Lourens, L.J., Rohling, E.J., 2015. Precession and obliquity forcing of the freshwater budget over the Mediterranean. Quat. Sci. Rev. 123, 16–30.

Broccoli, A.J., Dahl, K.A., Stouffer, R.J., 2006. Response of the ITCZ to northern hemisphere cooling. Geophys. Res. Lett. 33. L01702.

Burns, S.J., Welsh, L.K., Scroxton, N., Cheng, H., Edwards, R.L., 2019. Millennial and orbital scale variability of the South American Monsoon during the penultimate glacial period. Sci. Rep. 9, 1234.

Chiang, J.C.H., Bitz, C.M., 2005. Influence of high latitude ice cover on the marine Intertropical Convergence Zone. Clim. Dynam. 25, 477–496.

Cheng, H., Edwards, R.L., Broecker, W.S., Denton, G.H., Kong, X., Wang, Y., Zhang, R., Wang, X., 2009. Ice age terminations. Science 326, 248–252.

Cheng, H., Edwards, R.L., Wang, Y., Kong, X., Ming, Y., Kelly, M.J., Wang, X., Gallup, C.D., Liu, W., 2006. A penultimate glacial monsoon record from Hulu Cave and two-phase glacial terminations. Geology 34, 217–220.

Clews, J.E., 1989. Structural controls on basin evolution: Neogene to Quaternary of the Ionian zone, western Greece. J. Geol. Soc. 146, 447–457.

Colleoni, F., Wekerle, C., Näslund, J.-O., Brandefelt, J., Masina, S., 2016. Constraint on the penultimate glacial maximum Northern Hemisphere ice topography (~140 kyrs BP). Quat. Sci. Rev. 137, 97–112.

Corrick, E.C., Drysdale, R.N., Hellstrom, J.C., Capron, E., Rasmussen, S.O., Zhang, X., Fleitmann, D., Couchoud, I., Wolff, E., 2020. Synchronous timing of abrupt climate changes during the last glacial period. Science 369, 963–969.

Cortina, A., Sierro, F.J., Flores, J.A., Martrat, B., Grimalt, J.O., 2015. The response of SST to insolation and ice sheet variability from MIS 3 to MIS 11 in the northwestern Mediterranean Sea (Gulf of Lions). Geophys. Res. Lett. 42 (10), 366.

Cremer, H., Wagner, B., 2003. The diatom flora in the ultra-oligotrophic Lake El'gygytgyn, Chukotka. Polar Biol. 26, 105–114.

Dansgaard, W., Johnsen, S.J., Clausen, H.B., Dahl-Jensen, N., Gundestrup, S., Hammer, C.U., Hvidberg, C.S., Steffensen, J.P., Sveinbjörnsdottir, Jouzel, J., Bond, G., 1993. Evidence for general instability of past climate from a 250-kyr ice-core record. Nature 364, 218–220.

Deaney, E.L., Barker, S., van de Flierdt, T., 2017. Timing and nature of AMOC recovery across Termination 2 and magnitude of deglacial CO_2 change. Nat. Commun. 8, 14595.

Didié, C., Bauch, H.A., 2000. Species composition and glacial-interglacial variations in the ostracode fauna of the northeast Atlantic during the past 200,000 years. Mar. Microplaeontol. 40, 105–129.

Downing, G., 2008. Variability of North Atlantic Ice Rafting during the Last Two Glaciations. PhD Thesis. Columbia University.

Douglas, M.S.V., Smol, J.P., Blake Jr., W., 1994. Marked post 18th century environmental change in the high Arctic ecosystems. Science 266, 416–419.

Ehlers, J., Astakhov, V., Gibbard, P.L., Mangerud, J., Svendsen, J.I., 2013. Middle Pleistocene in Eurasia. In: Elias, S.A. (Ed.), Encyclopaedia of Quaternary Science. Elsevier, Amsterdam, pp. 172–179.

Ehlers, J., Gibbard, P.L., Hughes, P.D., 2018. Quaternary Glaciations and Chronology. In: Menzies, J., van der Meer, J. (Eds.), Past Glacial Environments (Sediments, Forms and Techniques), second ed. Elsevier, Amsterdam, pp. 77–101.

EPICA Community Members, 2006. One-to-one coupling of glacial climate variability in Greenland and Antarctica. Nature 444, 195–198.

Eynaud, F., Zaragosi, S., Scourse, J.D., Mojtahid, M., Bourillet, J.F., Hall, I.R., Penaud, A., Locascio, M., Reijonen, A., 2007. Deglacial laminated facies on the NW European continental margin: the hydrographic significance of British-Irish Ice Sheet deglaciation and Fleuve Manche paleoriver discharges. Geochemistry. Geophys. Geosystems 8. Q06019.

Fahnenstiel, G.L., Glime, J.M., 1983. Subsurface chlorophyll maximum and associated Cyclotella pulse in Lake Superior. Int. Rev. Gesamten Hydrobiol. 68, 605–616.

Frogley, M.R., Griffiths, H.I., Heaton, T.H.E., 2001. Historical biogeography and Late Quaternary environmental change of lake Pamvotis, Ioannina (north-western Greece): evidence from ostracods. J. Biogeogr. 28, 745–756.

Gibbard, P.L., West, R.G., Hughes, P.D., 2018. Pleistocene glaciation of Fenland, England, and its implications for evolution of the region. R. Soc. Open Sci. 4, 170736.

Gottschalk, J., Skinner, L.C., Misra, S., Waelbroeck, C., Menviel, L., Timmermann, A., 2015. Abrupt changes in the southern extent of North Atlantic deep water during Dansgaard-Oeschger events. Nat. Geosci. 8, 950–954.

Grant, K.M., Rohling, E.J., Bronk Ramsey, C., Cheng, H., Edwards, R.L., Florindo, F., Heslop, D., Marra, F., Roberts, A.P., Tamisiea, M.E., Williams, F., 2014. Sea-level variability over five glacial cycles. Nat. Commun. 5, 5076.

Grimm, E.C., 1987. CONISS: a FORTRAN 77 program for the stratigraphically constrained cluster analysis by the method of incremental sum of squares. Comput. Geosci. 13, 13–35.

Haworth, E.Y., 1976. Two late-glacial (Late Devensian) diatom assemblage profiles from northern Scotland. New Phytol. 77, 227–256.

Henry, L.G., McManus, J.F., Curry, W.B., Roberts, N.L., Piotrowski, A.M., Keigwin, L.D., 2016. North Atlantic Ocean circulation and abrupt climate change during the last glaciation. Science 353, 470–474.

Hoagland, K.D., Peterson, C.G., 1990. Effects of light and wave disturbance on vertical zonation of attached microalgae in a large reservoir. J. Phycol. 26, 450–457.

Hughes, P.D., Woodward, J.C., Gibbard, P.L., Macklin, M.G., Gilmour, M.A., Smith, G.R., 2006. The glacial history of the Pindus Mountains, Greece. J. Geol. 114, 413–434.

Hughes, P.D., Woodward, J.C., van Calsteren, P.C., Thomas, L.E., 2011. The glacial history of the dinaric Alps, Montenegro. Quat. Sci. Rev. 30, 3393–3412.

Hughes, P.D., Gibbard, P.L., 2018. Global glacier dynamics during 100 ka Pleistocene glacial cycles. Quat. Res. 90, 222–243.

Hughes, P.D., Gibbard, P.L., Ehlers, J., 2020. The "missing glaciations" of the middle Pleistocene. Quat. Res. 96, 161–183.

Jones, T.D., Lawson, I.T., Reed, J.M., Wilson, G.P., Leng, M.J., Gierga, M., Bernasconi, S.M., Smittenberg, R.H., Hajdas, I., Bryant, C.L., Tzedakis, P.C., 2013. Diatom-inferred late Pleistocene and Holocene palaeolimnological changes in the Ioannina basin, northwest Greece. J. Paleolimnol. 49, 185–204.

Jouzel, J., Masson-Delmotte, V., Cattani, O., Dreyfus, G., Falourd, S., Hoffmann, G., Minster, B., Nouet, J., Barnola, J.M., Chappellaz, J., Fischer, H., Gallet, J.C., Johnsen, S., Leuenberger, M., Loulergue, L., Luethi, D., Oerter, H., Parrenin, F., Raisbeck, G., Raynaud, D., Schilt, A., Schwander, J., Selmo, E., Souchez, R.,

Spahni, R., Stauffer, B., Steffensen, J.P., Stenni, B., Stocker, T.F., Tison, J.L., Werner, M., Wolff, E.W., 2007. Orbital and Millennial Antarctic climate variability over the past 800,000 years. Science 317, 793–796.
Kageyama, M., Merkel, U., Otto-Bliesner, B., Prange, M., Abe-Ouchi, A., Lohmann, G., Ohgaito, R., Roche, D.M., Singarayer, J., Swingedouw, D., Zhang, X., 2013. Climate impacts of fresh water hosing under Last Glacial Maximum conditions: a multi-model study. Clim. Past 9, 935–953.
Kaspi, Y., Sayag, R., Tziperman, E., 2004. A "triple sea-ice" mechanism for the abrupt warming and synchronous ice sheet collapses during Heinrich events. Paleoceanography 19. PA3004.
Koltai, G., Spötl, C., Shen, C.-C., Wu, C.-C., Rao, Z., Palcsu, L., Kele, S., Surányi, G., Bárány-Kevei, I., 2017. A penultimate glacial climate record from southern Hungary. J. Quat. Sci. 32, 946–956.
Krammer, K., Lange-Bertalot, H., 1986. Süsswasserflora Van Mitteleuropa. In: Bacillariophyceae. 1. Teil: Naviculaceae, 2/1. Gustav Fischer Verlag, Stuttgart.
Krammer, K., Lange-Bertalot, H., 1988. Süsswasserflora Van Mitteleuropa. In: Bacillariophyceae. 2. Teil: Epithemiaceae, Bacillariaceae, Surirellaceae, 2/2. Gustav Fischer Verlag, Stuttgart.
Krammer, K., Lange-Bertalot, H., 1991a. Süsswasserflora Van Mitteleuropa. In: Bacillariophyceae. 3. Teil: Centrales, Fragilariaceae, Eunotiaceae, 2/3. Gustav Fischer Verlag, Stuttgart.
Krammer, K., Lange-Bertalot, H., 1991b. Süsswasserflora Van Mitteleuropa. In: Bacillariophyceae. 4. Teil: Achnanthaceae, 2/4. Gustav Fischer Verlag, Stuttgart.
Kukla, G., An, Z.S., Melice, J.L., Gavin, J., Xiao, J.L., 1994. Magnetic susceptibility record of Chinese Loess. Trans. R. Soc. Edinb. Earth Sci. 81, 263–288.
Laing, T.E., Smol, J.P., 2003. Late Holocene environmental changes inferred from diatoms in a lake on the western Taimyr Peninsula, northern Russia. J. Paleolimnol. 30, 231–247.
Lambert, F., Delmonte, B., Petit, J.R., Bigler, M., Kaufmann, P.R., Hutterli, M.A., Stockler, T.F., Ruth, U., Steffensen, J.P., Maggi, V., 2008. Dust-climate couplings over the past 800,000 years from the EPICA Dome C ice core. Nature 452, 616–619.
Lambert, F., Bigler, M., Steffensen, J.P., Hutterli, M., Fischer, H., 2012. Centennial mineral dust variability in high-resolution ice core data from Dome C, Antarctica. Clim. Past 8, 609–623.
Leng, M.J., Marshall, J.D., 2004. Palaeoclimate interpretation of stable isotope data from lake sediment archives. Quat. Sci. Rev. 23, 811–831.
Levkov, Z., Krstic, S., Metzeltin, D., Nakov, T., 2007. Diatoms of Lakes Prespa and Ohrid. About 500 taxa from ancient lake system. Iconogr. Diatomol. v. 16. Gantner Verlag, Ruggell.
Li, C., Battisti, D.S., Schrag, D.P., Tziperman, E., 2005. Abrupt climate shifts in Greenland due to displacements of the sea ice edge. Geophys. Res. Lett. 32. L19702.
Lisiecki, L., Stern, J.V., 2016. Regional and global benthic $\delta^{18}O$ stacks for the last glacial cycle. Paleoceanography 31, 1368–1394.
Lolis, C.J., 2012. High-resolution precipitation over the southern Balkans. Clim. Res. 55, 167–179.
Lotter, A.F., Bigler, C., 2000. Do diatoms in the Swiss Alps reflect the length of ice-cover? Aquat. Sci. 62, 125–141.
Lotter, A.F., Pienitz, R., Schmidt, R., 1999. Diatoms as indicators of environmental change near arctic and alpine treeline. In: Stoermer, E.F., Smol, J.P. (Eds.), The Diatoms: Applications for the Environmental and Earth Sciences. Cambridge University Press, Cambridge, pp. 205–226.
Lynch-Stieglitz, J., 2017. The Atlantic meridional overturning circulation and abrupt climate change. Ann. Rev. Mar. Sci. 8, 83–104.
Margari, V., Skinner, L.C., Tzedakis, P.C., Ganopolski, A., Vautravers, M., Shackleton, N.J., 2010. The nature of millennial-scale climate variability during the past two glacial periods. Nat. Geosci. 3, 127–131.
Margari, V., Skinner, L.C., Hodell, D.A., Martrat, B., Toucanne, S., Grimalt, J.O., Gibbard, P.L., Lunkka, J.P., Tzedakis, P.C., 2014. Land-ocean changes on orbital and millennial time scales and the penultimate glaciation. Geology 42, 183–186.
Martrat, B., Jimenez-Amat, P., Zahn, R., Grimalt, J.O., 2014. Similarities and dissimilarities between the last two deglaciations and interglaciations in the North Atlantic region. Quat. Sci. Rev. 99, 122–134.
Martrat, B., Grimalt, J.O., Shackleton, N.J., de Abreu, L., Hutterli, M.A., Stocker, T.F., 2007. Four climate cycles of recurring deep and surface water destabilizations on the Iberian margin. Science 317, 502–507.
Martrat, B., Grimalt, J.O., Lopez-Martinez, C., Cacho, I., Sierro, F.J., Abel Flores, J., Zahn, R., Canals, M., Curtis, J.H., Hodell, D.A., 2004. Abrupt temperature changes in the Western Mediterranean over the past 250,000 years. Science 306, 1762–1765.
McManus, J.F., Oppo, D.W., Cullen, J.D., 1999. A 0.5-million-year record of millennial-scale climate variability in the North Atlantic. Science 283, 971–975.
Nagavciuc, V., Badaluta, C.-A., Ionita, M., 2019. Tracing the relationship between precipitation and river water in the northern Carpathians based on the evaluation of water isotope data. Geosciences 9 (5), 198.
Nehme, C., Verheyden, S., Breitenbach, S.F.M., Gillikin, D.P., Veŕheyden, A., Cheng, H., Edwards, R.L., Hellstrom, J., Noble, S.R., Farrant, A.R., Sahy, D., Goovaerts, T., Salem, G., Claeys, P., 2018. Climate dynamics during the penultimate glacial period recorded in a speleothem from Kanaan Cave, Lebanon (central Levant). Quat. Res. 90, 10–25.
Obrochta, S.P., Crowley, T.J., Channell, J.E.T., Hodell, D.A., Baker, P.A., Seki, A., Yokoyama, Y., 2014. Climate variability and ice-sheet dynamics during the last three glaciations. Earth Planet Sci. Lett. 406, 198–212.
Ohlendorf, C., Bigler, C., Goudsmit, G.-H., Lemcke, G., Livingstone, D.M., Lotter, A.F., Müller, B., Sturm, M., 2000. Cause and effects of long periods of ice cover on a remote high Alpine lake. J. Limnol. 59 (Suppl. 1), 65–80.
Pedro, J.B., Jochum, M., Buizert, C., He, F., Barker, S., Rasmussen, S.O., 2018. Beyond the bipolar seesaw: toward a process understanding of interhemispheric coupling. Quat. Sci. Rev. 192, 27–46.
Rawlence, D.J., 1992. Paleophycology of Long Lake, Saint John County, New Brunswick, Canada, based on diatom distribution in sediments. Can. J. Bot. 70, 229–239.
Regattieri, E., Zanchetta, G., Drysdale, R.N., Isola, I., Hellstrom, J.C., Roncioni, A., 2014. A continuous stable isotope record from the penultimate glacial maximum to the Last Interglacial (159-121 ka) from Tana Che Urla Cave (Apuan Alps, central Italy). Quat. Res. 82, 450–461.
Rhodes, R.H., Brook, E.J., Chiang, J.C.H., Blunier, T., Maselli, O.J., McConnell, J.R., Romanini, D., Severinghaus, J.P., 2015. Enhanced tropical methane production in response to iceberg discharge in the North Atlantic. Science 348, 1016–1019.
Roucoux, K.H., Tzedakis, P.C., Lawson, I.T., Margari, V., 2011. Vegetation history of the penultimate glacial period (MIS 6) at Ioannina, north-west Greece. J. Quat. Sci. 26, 616–626.
Rühland, K., Paterson, A.M., Smol, J.P., 2008. Hemispheric-scale patterns of climate-related shifts in planktonic diatoms from North America and European lakes. Global Change Biol. 14, 2740–2754.
Rühland, K., Paterson, A.M., Smol, J.P., 2015. Lake diatom responses to warming: reviewing the evidence. J. Paleolimnol. 54, 1–35.
Ruth, U., Bigler, M., Rothlisberger, R., Siggaard-Andersen, M.L., Kipfstuhl, S., Goto-Azuma, K., Hansson, M.E., Johnsen, S.J., Lu, H.Y., Steffensen, J.P., 2007. Ice core evidence for a very tight link between North Atlantic and east Asian glacial climate. Geophys. Res. Lett. 34 (3). L03706.
Schmidt, R., Kamenik, C., Lange-Bertalot, H., Klee, R., 2004. *Fragilaria* and *Staurosira* (Bacillariophyceae) from sediment surfaces of 40 lakes in the Austrian Alps in relation to environmental variables, and their potential for palaeoclimatology. J. Limnol. 63, 171–189.
Smol, J.P., Wolfe, A.P., Birks, J.H.B., Douglas, M.S.V., Jones, V.J., Korhola, A., Pienitz, R., Rühland, K.M., Sorvari, S., Antoniades, D., Brooks, S.J., Fallu, M.-A., Hughes, M., Keatley, B.E., Laing, T.E., Michelutti, N., Nazarova, L., Nyman, M., Peterson, A.M., Perren, B., Quinlan, R., Rautio, M., Saulnier-Talbot, E., Siitonen, S., Solovieva, N., Weckström, J., 2005. Climate-driven regime shifts in the biological communities of arctic lakes. Proc. Natl. Acad. Sci. Unit. States Am. 102, 4397–4402.
Toucanne, S., Zaragosi, S., Bourillet, J.F., Cremer, M., Eynaud, F., Van Vliet-Lanoë, Penaud, A., Fontanier, C., Turon, J.L., Cortijo, E., Gibbard, P.L., 2009. Timing of massive 'Fleuve Manche' discharges over the last 350 kyr: insights into the European ice-sheet oscillations and the European drainage network from MIS 10 to 2. Quat. Sci. Rev. 28, 1238–1256.
Treidl, R.A., Birch, E.C., Sajecki, P., 1981. Blocking action in the northern hemisphere: a climatological study. Atmos.-Ocean 19 (1), 1–23.
Tzedakis, P.C., Frogley, M.R., Heaton, T.H.E., 2003. Last interglacial conditions in southern Europe: evidence from Ioannina, northwest Greece. Global Planet. Change 36, 157–170.
Tzedakis, P.C., Pälike, H., Roucoux, K.H., de Abreu, L., 2009. Atmospheric methane, southern European vegetation and low-mid latitude links on orbital and millennial timescales. Earth Planet Sci. Lett. 277, 307–317.
Tzedakis, P.C., Lawson, I.T., Frogley, M.R., Hewitt, G.M., Preece, R.C., 2002. Buffered tree population changes in a Quaternary refugium: evolutionary implications. Science 297, 2044–2047.
Tzedakis, P.C., Drysdale, R.N., Margari, V., Skinner, L.C., Menviel, L., Rhodes, R.H., Tashetto, A.S., Hodell, D.A., Crowhurst, S.J., Hellstrom, J.C., Fallick, A.E., Grimalt, J.O., McManus, J.F., Martrat, B., Mokeddem, Z., Parrenin, F., Regattieri, E., Roe, K., Zanchetta, G., 2018. Enhanced climate instability in the North Atlantic and southern Europe during the last interglacial. Nat. Commun. 9, 4235.
Waltham, A.C., 1970. The karstlands of the Ioannina region, NW Greece. J. British Spel. Assoc. 6, 1–11.
Wagner, B., Vogel, H., Francke, A., et al., 2019. Mediterranean winter rainfall in phase with African monsoons during the past 1.36 million years. Nature 573, 256–260.
Wang, Q., Wang, Y., Shao, Q., Liang, Y., Zhang, Z., Kong, X., 2018. Millennial-scale Asian monsoon variability during the late Marine Isotope Stage 6 from Hulu cave, China. Quat. Res. 90, 394–405.
Wang, X., Auler, A.S., Edwards, R.L., Cheng, H., Cristalli, P.S., Smart, P.L., Richards, D.A., Shen, C.-C., 2004. Wet periods in northeastern Brazil over the past 210 kyr linked to distant climate anomalies. Nature 432, 740–743.
Wang, Y., Cheng, H., Edwards, R.L., Kong, X., Shao, X., Chen, S., Wu, J., Jiang, X., Wang, X., An, Z., 2008. Millennial- and orbital-scale changes in the East Asian monsoon over the past 224,000 years. Nature 451, 1090–1093.
Wang, Q., Yang, X., Hamilton, P.B., Zhang, E., 2012. Linking spatial distributions of sediment diatom assemblages with hydrological depth profiles in a plateau deep-water lake system of subtropical China. Fottea 12, 59–73.
Wilson, G.P., Reed, J.M., Frogley, M.R., Hughes, P.D., Tzedakis, P.C., 2015. Reconciling diverse lacustrine and terrestrial system response to penultimate deglacial warming in southern Europe. Geology 43, 819–822.
Wilson, G.P., Reed, J.M., Lawson, I.T., Frogley, M.R., Preece, R.C., Tzedakis, P.C., 2008. Diatom response to the last glacial-interglacial transition in the Ioannina basin, northwest Greece: implications for Mediterranean palaeoclimate reconstruction. Quat. Sci. Rev. 27, 428–440.
Wilson, G.P., Frogley, M.R., Roucoux, K.H., Jones, T.D., Leng, M.J., Lawson, I.T., Hughes, P.D., 2013. Limnetic and terrestrial responses to climate change during the onset of the penultimate glacial stage in NW Greece. Glob. Planet. Change 107 213–225.
Winder, M., Reuter, J.E., Schladow, S.G., 2009. Lake warming favours small-sized planktonic diatom species. Proc. Royal Soc. B 276, 427–435.
Zhang, R., Delworth, T.L., 2005. Simulated tropical response to a substantial weakening of the Atlantic thermohaline circulation. J. Clim. 18, 1853–1860.